Hydrology and Earth System Sciences

Open Access

Discussions

Impacts of climate change under CMIP5 RCP scenarios on the streamflow in the Dinder River and ecosystem habitats in Dinder National Park, Sudan

A. K. Basheer[1,2], H. Lu[1], A. Omer[1], A. B. Ali[3], and A. M. S. Abdelgader[4]

[1]State Key Laboratory of Hydrology-Water Resources and Hydraulic Engineering, College of Hydrology and Water Resources, Hohai University, Nanjing, 210098, China
[2]Ministry of Agriculture and Irrigation, River Nile State, P.O. Box 8168, Adamar, 12217, Sudan
[3]College of Water Conservancy and Hydropower, Hohai University, Nanjing, 210098, China
[4]School of information science and Eng. Southeast University, Nanjing, 210096, China

Correspondence to: H. Lu (haishenlu@gmail.com)

HESSD

Impacts of climate change under CMIP5 RCP scenarios on the streamflow in the Dinder River

A. K. Basheer et al.

Title Page

Abstract	Introduction
Conclusions	References
Tables	Figures

|◄ | ►|
◄ | ►

Back | Close

Full Screen / Esc

Printer-friendly Version

Interactive Discussion

Abstract

The fate of seasonal rivers ecosystem habitats under climate change essentially depends on the changes in annual recharge, which related to alterations in precipitation and evaporation over the river basin. Therefore the change in climate conditions is expected to significantly affect hydrological and ecological components, particularly in fragmented ecosystems. This study aims to assess the impacts of climate change on the streamflow in Dinder River Basin (DRB), and infer its relative possible effects on the Dinder National Park (DNP) ecosystem habitats in the Sudan. Two global circulation models (GCMs) from Coupled Model Intercomparison Project Phase 5 and two statistical downscaling approaches combined with hydrological model (SWAT) were used to project the climate change conditions over the study periods 2020s, 2050s and 2080s. The results indicated that the climate over the DRB will become warmer and wetter under the most scenarios. The projected precipitation variability mainly depends on the selected GCM and downscaling approach. Moreover, the projected streamflow was more sensitive to rainfall and temperature variation, and will likely increase in this century. In contrast to drought periods during (1960s, 1970s and 1980s), the predicted climate change is likely to affect ecosystems in DNP positively and promote the ecological restoration of the flora and fauna habitats'.

1 Introduction

The climate change over the next century expected to severely impact water resources; arid and semi-arid areas are particularly more vulnerable to that change and projected to suffer from water shortage due to precipitation reduction (Tavakoli and De Smedt, 2011; Setegn et al., 2011). Alteration in hydrologic conditions will affect almost every aspect of natural resources and human well-being (Xu, 1999). For instance, ecosystem integrity is influenced either directly or indirectly by climate change and hydrologic variability globally, regionally and at catchments' scale. The responses of ecosystems

to alterations in the hydrological process usually include complex interactions of biotic and abiotic processes. Hence, the hydrological variability can highly impact the ecosystem species in a variety of ways, such as the linkage between water availability and metabolic and reproductive processes of that species (Burkett et al., 2005). Among all ecosystems, freshwater ecosystem is seriously expected to affect species, which mainly caused by climate change (Millennium Ecosystem Assessment, 2005). Both current climate (maximum temperature) and climate change (precipitation change) appear to be key determinants of habitat loss and fragmentation effects on terrestrial biodiversity (Mantyka-pringle et al., 2012). In some part of the world, ecosystems are already being affected by climate variability. Furthermore, it is very likely that the magnitude and frequency of ecosystem changes will possible rapidly increase and continue in the future (Thomas et al., 2004). As the climate conditions have changed in both precipitation and temperature trends over recent decades, the timing of these events has become vulnerable for alteration as well. According to the Gitay et al. (2002) projections, the ecosystem components in the Northern Hemisphere will experience serious alterations in terms of earlier flowering of plants, migration of birds, animal breeding seasons and emergence of insects. Consequently, under the smallest climatic change scenarios, 18 % of species were found to be "committed to extinction" while the largest change scenario projected as many as 35 % of species to be at risk (Thomas et al., 2004). Many studies investigated the impact of the streamflow change on the freshwater ecosystems, which will probably have strong effects on the system components and abiotic characteristic (Poff and Ward, 1989; Poff and Zimmerman, 2010; Döll and Zhang, 2010; Mantyka-pringle et al., 2012). Erwin (2009) concluded that the wetlands will a strongly be influenced due to climate alteration and to overcome all these impact firstly assessment of the affect should be conducted. These assessments should be applied, particularly in semi-arid and arid regions which will be more vulnerable areas (Finlayson et al., 2006). The Dinder River (DR) is one of the largest tributary of the Blue Nile River and major water resources in the Dinder National Park (DNP). It seasonally flows down from western parts of the Ethiopian highlands and flows through the centre

of the DNP (Abdel Hameed et al., 1997). Seasonality of DR makes it more sensitive to climate change effects, because it mainly depends on seasonal rainfall, which expected to be altered in timing and magnitude. On the other hand, ecosystem habitats in the Dinder river basin (DRB) is basically controlled by the river runoff and climate variables such as temperature and precipitation. Whereas, DNP biodiversity is related to high flow events of DR that influence the river channel shape and allow access to other disconnect floodplain habitats, and to low flow events that limit overall habitats availability and quality. Ecosystem in DNP contains a group of islands, and wetlands (Mayas) consist of a diverse array of fauna and flora and represent adequate environment for most nutritious grasses to the herbivores, especially during the most severe part of the dry season. Thus, relative changes in hydrological process and climate variables over DRB directly affect the ecosystem habitats and components in the DNP as general.

In order to evaluate the effects of climate change on natural resources, technical measurements and researches should be conducted within the context of water resources management and maintaining ecosystem integrity at the local and territorial scales. One of the best tools for simulating current and future prediction of climate change scenarios is GCMs (Xu, 1999). However, there is a general consensus among the scientific community that GCM outputs cannot be used directly as input to hydrological models, which often operate on spatial scales smaller than those of GCMs (Wilby et al., 2002). To predict changes in hydrology and water resources, downscaling the outputs of the GCM on the global scale into the inputs of the hydrological model on the regional scale has been widely applied to obtain the hydrological response (Charlton et al., 2006; Steele-Dunne et al., 2008). Statistical downscaling is thus often used to bridge the scale gap in linking GCM outputs with hydrological models because it does not require significant computing resources and can more directly incorporate observations into method (Fowler et al., 2007). The hydrologic models should provide a link between climate changes and water yields through simulation of hydrologic processes within watersheds. Notwithstanding, most hydrologic models are unable to incorporate

the climate change effect for simulation. The Soil and Water Assessment Tool (SWAT) is one of the widely used model which has the capability of incorporating the climate change effect for simulation (Ficklin et al., 2010).

Up to the authors' knowledge, the impact of climate change in DRB has not been thoroughly projected and explicitly explored by which of these hydrological alteration, the DNP wetland habitats can be affected. Investigation of the ecosystem habitats response to climate change is hard to achieve at a sufficient scale. However, the climatic impact and hydrological alteration could potentially have large effect on ecosystem habitats need to be considered.

The objectives of this paper are: (1) assess the climate change effect on the future streamflow magnitude of the DRB, using SWAT coupled with two GCMs under various climate change scenarios and two downscaling approaches, (2) investigation of the potential impacts of climate change on the DNP ecosystem components, in order to provide benchmarked information for the decision-makers to be included in adaptation strategies for water resources and environment sustainable development. The rest of the paper is organized as follows. Section 2 describes the study area including climate, hydrology and DNP ecosystem components. This is followed by a brief description of the SWAT model and two downscaling approaches used to downscale the GCMs model outputs. Section 4 provides the results and discussion of the projected climate variables and streamflow when applying two methods and investigates their affect on the ecosystem habitats. Section 6 concludes this works.

2 Materials and methods

2.1 Study area

Dinder River Basin (DRB) is the largest tributary of the Blue Nile in Sudan. It has a seasonal character where it starts surging in June, peaking around the middle of August each year, and in normal conditions ceases flowing in November. The entire

basin ranges in elevation from 2646 m at an Ethiopian plateau to 515 m at the north-west point where it joined the Blue Nile and its catchments' area about 31 422 km^2. DRB geographic coordination is 11°41′ to 13°85′ N and 34 to 36°20′ E. The average annual discharge for the previous 40 years at the Al Gwisi hydrological station is about

5 1.9 billion m^3 (BCM), with seasonal variation ranged between 151 % (4.78 BCM) increment in the wettest year and 65 % (0.35 BCM) decrease in the dry year. This high variability of the runoff is due to the significant rainfall alteration over the basin. The main land use and land cover classes in DRB are agriculture, forest, grass, bush, shrubs and others (Abdel Hameed, 1983; Abdel Hameed and Eljack, 2003). Land use of the study

10 area has changed over time due to over increasing population density and agricultural practices. The clay plains of DRB are probably the most striking feature of the geo-morphology of Sudan (Whiteman, 1971). There are some types of soil in DRB such as *Eutric Cambisols*, *Chromic Cambisols*, *Eutric Gleysols*, *Eutric Regosols*, *Chromic Vertisols* and *Pellic Vertisols*. The sandy river bed is left with only a few pools (Mayas)

15 which may hold water up to the next rainy season after it ceases to flow (Abdel Hameed, 1983). The annual rainfall amount is normally increased gradually from 500 mm in the north-western part to 1110 mm in the south-eastern part. The DRB drainage system contains of four sub-drainages namely Khor Galegu drainage system, which is the biggest tributary of the Dinder River, Khor Masaweek, East bank of river Dinder and

20 West bank of river Dinder. Each one of these sub-drainages consists of a number of Mayas, which mainly fed by the main DR stream and its tributaries through distinct feeder channels according to the amount of overflow of the river in flood months (Abdel Hameed et al., 1997).

2.2 Dinder national park ecosystem

25 Dinder national park is considered one of the largest natural reserves in northeast Africa, which was proclaimed as a national park in 1935 following the London Convention (Dasmann, 1972) for the conservation of African flora and fauna. It is located in the southeast Sudan between longitude 34°30′ and 36°00′ E and latitude 11°00′

and 13°00′ N, covering an area of 10 846 km^2. DNP is the only national park north of the 10 parallel, which forms an important ecological zone in the arid and semi-arid Sudano-Saharan region. It has high elevation variation ranges from 2646 m at an Ethiopian Plateau to about 515 m at the south-eastern part and 100 m at north-eastern part. The Park has unique biodiversity contain a variety with over 250 species of birds, 27 species of large mammals; some of them are listed by the International Union for Conservation of Nature (IUCN) as endangered, vulnerable or threatened species, in addition to an unknown number of smaller mammals. Therefore, the park is considered as adequate habitation for a large number of animals during the dry season and a few numbers when it rains from June through October. The Mammalian fauna leave the Mayas of the park during the rainy season to the high grounds at the east part, in Ethiopia and return with the onset of the dry season. The Mayas are formed by meanders and oxbows along the rivers. It provides dwelling and support for a large number of animal species, such as tiang (*Damaliscus korrigum*), lion (*Panthera leo*), Elephant (*Loxodonta africana*, leopard (*Panthera pardus*), wild dog (*Lycaon pictus*), the red–fronted gazell (*Gazella rufifrons*), greater kudu (*Tragelaphus strepsicerus*), Nubian giraffe (*Giraffa camelopardalis*), black-backed jackal (*Conis mesomelas*), Arabian bustard and greater bustard. There are also numerous hides of insects, which serve a vital function in recycling of the organic compounds (Abdel Hameed and Eljack, 2003).

2.3 The hydrological model (SWAT)

SWAT is a continuous, long-term, distributed-parameter hydrological model designed to predict the impact of land management practices on the hydrology and sediment and contaminant transport in agricultural watersheds (Arnold et al., 1998). SWAT subdivides a watershed into sub-basins connected by a stream network, and further delineates hydrologic response units (HRUs) consisting of unique combinations of land cover and soils within each sub-basin. The model assumes that there are no interactions among HRUs, and these HRUs are virtually located within each sub-basin. HRUs

delineation minimizes the computational costs of simulations by lumping similar soil and land use areas into a single unit (Neitsch et al., 2002). A detailed description of the basin scale of hydrological model (SWAT) can be found in many literature such as Neitsch et al. (2005a, b).

Input data preparation

In addition to meteorological data, the model simulation required a range of spatially distributed data such as topographic features, soil types, land use and the stream network (optional). Digital Elevation Model (90 m, USGS) (Fig. 1) was used to delineate the watershed and the drainage patterns of the surface area analysis. Daily meteorological data, such as temperature and precipitation were collected from Ministry of Water resources and Electricity and Nile Basin Initiative for the period 1961 to 2008. These data are interpolated from meteorological stations distributed within the Blue Nile River Basin. Moreover, daily records of the river discharge at the Al Gwisi hydrological station were obtained from the Ministry of Water Resources and Electricity of Sudan. Land use map in this study was obtained from the land cover institute (LCI) (http://landcover.usgs.gov/) and other field classification for the study area. The soil map for the study area extracted from the digital soil map of the world (FAO) and African soil map.

2.4 Global circulation model selection

The projected temperature and precipitation were obtained from the IPCC Data Distribution Centre (http://cmip-pcmdi.llnl.gov/cmip5/). Two GCMs have been selected in this study as shown in Table 1. The MPI-ESM-LR model which developed by the Max-Planck-Institute for Meteorology, Hamburg, Germany, and the CCSM4 model developed by the National Centre for Atmospheric Research. Representative concentration pathway (RCP4.5 and RCP8.5) forcing climate scenarios were selected based on the two GCMs. The daily precipitation, maximum and minimum temperature from 1961 up

to 2095 were extracted from grid cells covering DRB. The period from 1961–1990 was defined as the baseline period (denoted by 1980s). While the future periods which covered by this study are 2006–2035, 2036–2065 and 2066–2095 (denoted by the 2020s, 2050s and 2080s, respectively), except precipitation for CCSM4 model under RCP8.5 scenario (2066–2093).

3 Methodology

3.1 Streamflow simulation and calibration

SWAT was used to simulate streamflow in DRB. SWAT provides two methods for estimating surface runoff; the SCS curve number and the Green-Ampt infiltration method. The model calculates the peak runoff rate with a modified rational method (Chow et al., 1988). An automated calibration technique with Sequential Uncertainty Fitting Version 2 (Abbaspour et al., 2007) was used to calibrate the simulated streamflow at the Algwisi station in the DRB. Sensitive initial and default parameters related to hydrology were changed concurrently until an optimal solution was met. The coefficient of determination (R^2), and the Nash–Sutcliffe coefficient (Nash and Sutcliffe, 1970) were used to assess the model performance.

3.2 Statistical downscaling of temperature and rainfall time series

The GCMs outputs resolution is too coarse for regional impact assessment study; therefore, downscaling must be performed before applying GCM outputs into the SWAT model (Dessu and Melesse, 2013). Both change factor (CF) and quantile mapping (QM) downscaling methods were used to downscale GCM outputs.

3.2.1 Change factor downscaling method (CF)

In general, the CF method (Hay et al., 2000; Diaz-Nieto and Wilby, 2005) is an ordinary bias correction method. The CF method is often used to exclude or minimize the bias between observations and the model outputs. The CF procedures rely on modifying the daily time step series of the climate variables such as precipitation and temperature for prediction periods (2020s, 2050s and 2080s) by adding the monthly mean changes of GCM outputs. The adjusted formulas which are used to modify daily temperature and precipitation are expressed in Eqs. (1) and (2).

$$T_{\text{adj; fur; d}} = T_{\text{obs; d}} + \sum_{i=1}^{k} pi \left(\overline{T}_{\text{GCM; fur; m}} - \overline{T}_{\text{GCM; ref; m}} \right) \tag{1}$$

$$P_{\text{adj; fur; d}} = P_{\text{obs; d}} \times \sum_{i=1}^{k} pi \left(\overline{P}_{\text{GCM; fur; m}} / \overline{P}_{\text{GCM; ref; m}} \right) \tag{2}$$

where $T_{\text{adj; fur; d}}$ is the adjusted daily temperature ($T_{\max}$ and $T_{\min}$) for the future years, $T_{\text{obs; d}}$ is the observed daily temperature for the baseline years, $T_{\text{GCM; fur; m}}$ is the monthly mean temperature of the GCM outputs for the future years, $T_{\text{GCM; ref; m}}$ is the monthly mean temperature of the GCM outputs for the baseline years, pi is the weight of each grid cell and k is the number of the grid cells.

3.2.2 Quantile mapping downscaling method (QM)

Quantile mapping is an emerging downscaling approach that utilized to remove bias of observed and simulated rainfall using cumulative distribution functions (CDF). QM basically replaces the simulated (GCMs) rainfall value with the observed value that has the same non-exceedance probability. It shifts the occurrence distributions of precipitation through creating a transfer function (Sennikovs and Bethers, 2009; Teutschbein and Seibert, 2012). The recommended function for distributions of precipitation events is the Gamma distribution (Thom, 1958) as shown in Eq. (3).

$$f\gamma\left(x/\alpha,\beta\right) = x^{\alpha-1} \cdot \frac{1}{\beta^{\alpha} \cdot \Gamma(\alpha)} \cdot e^{\frac{-x}{\beta}}; \quad x \geq 0; \quad \alpha, \beta > 0 \tag{3}$$

where α is Shape parameter of Gamma distribution, β is Scale parameter of Gamma distribution, f is Distribution function, e is Euler's number, Γ is Gamma function and x is Independent (random) variable.

In this study, we used an advanced version of QM approach developed recently by Willems et al. (2012). The CDFs were set up on a daily basis for observed and the GCM-simulated rainfall for the baseline period (1961–1990). Then the GCM outputs value of a certain day was looked up based on the constructed CDF relative to the GCM simulations with their corresponding cumulative probability. Subsequently, the same cumulative probability of the precipitation value was located on the empirical CDF of observations. Then, this value was used to adjust the GCM baseline simulation (1961–1990). The Gamma CDF ($F\gamma$) and its inverse ($F\gamma - 1$) can elucidate this procedure mathematically as follows:

$$P_{\text{basper}}^{*}(d) = F_{\gamma}^{-1}(F_{\gamma}(P_{\text{basper}}(d)|\alpha_{\text{basper, d}}\ \beta_{\text{basper, d}})|\alpha_{\text{obs, d}}\ \beta_{\text{obs, d}}) \tag{4}$$

$$P_{\text{fut}}^{*}(d) = F_{\gamma}^{-1}(F_{\gamma}(P_{\text{fut}}(d)|\alpha_{\text{fut, d}},\ \beta_{\text{fut, d}})|\alpha_{\text{obs, d}},\ \beta_{\text{obs, d}}) \tag{5}$$

where P_{basper}^{*} is precipitation bias corrected for the base period of GCM, P_{fut}^{*} is precipitation bias corrected for the future period of GCM, F is a cumulative distribution function (CDF), F_{γ}^{-1} is the inverse of (CDF), γ is gamma distribution (Willems et al., 2012).

The difference between the two downscaling approaches is that CF method can obtain daily future precipitation time series by adding the average monthly changes of GCM outputs to the observed data. Conversely, QM approach directly adjusted the daily time series generated by the GCM based on linkage of GCM outputs and observed data in the baseline period.

Title Page

Abstract | Introduction

Conclusions | References

Tables | Figures

◄ | ►

◄ | ►

Back | Close

Full Screen / Esc

Printer-friendly Version

Interactive Discussion

4 Results and discussions

4.1 Calibration and validation for SWAT model

Firstly, SWAT was calibrated for the whole basin during the period 1989–1993 based on daily and monthly stream flow at the Al Gwisi hydrological station and the model inputs. Then, the model further validated over the period 1995–1999. Results showed that SWAT could successfully simulate reasonable daily and monthly streamflow in the DRB as shown in Fig. 2. Particularly, the coefficient of determination (R^2) and Nash–Sutcliffe coefficient of efficiency values (NSE) between monthly observed and simulated streamflow were 0.83 and 0.81 for the calibration period and 0.82 and 0.76 during the validation period, respectively. For the daily stimulation, R^2 and NSE values were 0.63 and 0.61 for the calibration period and 0.56 and 0.51 for the validation period as listed in Table 2. According to the criteria of Moriasi et al. (2007), SWAT model in the DRB shows acceptable performance.

4.2 Future climate change

CF and QM methods were employed to downscale the climate variables for the selected GCMs. In particular, the temperature data were downscaled using the CF approach, whereas the precipitation was downscaled using the two approaches.

4.2.1 Mean of T_{max} and T_{min}

The future climate conditions were determined using the combination of climate change scenarios (RCP4.5 and RCP8.5) and GCMs (MPI-ESM-LR and CCSM4). Figure 3 represents the difference between maximum and minimum temperature in the future and the baseline period (1961–1990). ESM indicates to the MPI-ESM-LR model; while CCSM represents the CCSM4 model, and RCP4.5 and RCP8.5 demonstrate the climate change scenarios. For instance; ESM4.5 shows the climate condition simulated by the MPI-ESM-LR model under the RCP4.5 climate change scenario. The maximum

temperature (T_{max}) trend analysis shows an obvious increment in the future. However, the change amplitude of T_{max} is uncertain due to differences in the applied GCMs models and scenarios. Annual average temperature increases ranges are between 0.9 to 1.6 °C, 1.5 to 2.9 °C and 1.7 to 4.9 °C in 2020s, 2050s and 2080s respectively, as shown in Table 3. Moreover, the RCP8.5 scenario predicted higher temperature increases than that of RCP4.5 during the study periods. Under the same climate change scenario (RCP4.8 and RCP8.5), MPI-ESM-LR model projected higher temperature increases than CCSM4 model in 2020s, 2050s and 2080s. Whereas, 2080s period showed the highest increase change in temperature based on the two models. The magnitude of the monthly temperature increment showed more variation under MPI-ESM-LR model with increase ranges from 0.8 to 3.9 °C, from 1.8 to 3.9 °C and from 2.2 to 6.2 °C in 2020s, 2050s and 2080s respectively. The temperature change in CCSM4 model fluctuated between −2.2 to 4.5 °C in 2020, from −0.9 to 4.2 °C in 2050s and from 0.1 to 5.7 °C in 2080s.

The projected annual minimum temperature (T_{min}) variability showed a marked upward trend overall periods and GCMs and scenarios as demonstrated in Fig. 3 and Table 4. Annual average minimum temperature increases ranged from 0.9 to 1.6 °C, from 1.6 to 3 °C and from 1.7 to 5.1 °C in 2020s, 2050s and 2080s respectively. Variation in monthly temperature showed more fluctuation in MPI-ESM-LR model, with a range from 1.1 to 2 °C, from 2 to 3.4 °C and from 2.5 to 5.9 °C in 2020s, 2050s and 2080s respectively. The CCSM4 model temperature change ranged from −1.4 to 2.1, from −0.02 to 2.1 and from 0.9 to 3.8 in 2020s, 2050s and 2080s respectively. Broadly, the expected temperature under different climate changes scenarios and conditions indicate that the overall climate will become much warmer as time passes. As shown in Table 4 the RCP8.5 scenario projected higher temperature increases than the RCP4.5 scenario in the whole periods. The MPI-ESM-LR model under the same climate change scenario (RCP4.8 and RCP8.5) predicted higher temperature increases than the CCSM4 model in the over study periods. Furthermore, 2080s period realized more temperature increase change in the two GCMs.

4.2.2   Mean precipitation

Figure 4 and Table 5 illustrate the projected change in annual precipitation under two GCMs and scenarios (RCP4.5 and RCP8.5), using CF and QM downscaling approaches. Mean annual precipitation projected by CCSM4 model showed a dramatic increase when CF method is applied, while MPI-ESM-LR model showed a significant upward trend during the same period. According to MPI-ESM-LR model, the mean annual precipitation changes ranged from 2.3 to 4.6 %, from 1.5 to 9.2 % and from 3 to 10.5 % in 2020s, 2050s and 2080s respectively, whereas CCSM4 model changes ranged from 40.4 to 42.5 %, from 35.3 to 39.7 % and from 28.1 to 36.2 % in 2020s, 2050s 2080s respectively. Conversely mean annual precipitation projected using the QM method showed a convergent significant upward trend under the two models, as it is clearly shown in MPI-ESM-LR model prediction, which indicates an increase trend ranged between 6.5 to 14.9 % in 2020s, 2050s and 2080s. The CCSM4 model showed increment ranged between 6.7 to 16.4 % over the study periods. Despite annual precipitation predicted by MPI-ESM-LR model under RCP8.5 scenario was displayed convergent upward trend under the two downscaling methods, its distribution and amount were varied at the monthly and daily scale. The variation in the obtained downscaling results is because of the characteristic variability of CF and QM approaches. In case of applying the CF approach, any decrease/increase in daily rainfall series will be as a consequence of a decrease/increase in the monthly precipitation. However, in the QM approach, the rainfall time series for the future period are taken from the GCM scenarios. The QM approach might predict an increment in maximum daily rainfall value, if a decrease in monthly precipitation is projected by GCM as shown by Camici et al. (2013).

Figure 5a displays the relationship between the mean daily rainfall projected by two downscaling approaches and GCMs outputs for the study periods. As it is shown, there is no such big difference between rainfall projections by two downscaling methods and MPI-ESM-L outputs. Accordingly, there is an insignificant change in projected mean

daily rainfall when two downscaling methods were used. Conversely, high variation was detected in mean daily rainfall when the CF approach applied corresponding to CCSM4 outputs, whereas QM prediction varied slightly when applied. Moreover, the correlation between the mean daily rainfall projected by the CF, QM approaches and baseline period corresponding to the GCM outputs illustrated by Fig. 5b. Obviously, the QM showed high correlation to GCMs outputs compared with the CF method. Furthermore, Fig. 5c demonstrates the variance of the mean daily rainfall generated by CF and QM relative to the simulations of the two GCMs. It is clearly there is a remarkable variance in mean daily rainfall provided by CCSM4 outputs compare with downscaled rainfall when the CF approach was applied.

From the results, there is uncertainty in projected temperature and precipitation due to the applied GCMs and downscaling approaches. Consequently, an uncertainty would be emerged in the predictions of future streamflow response.

4.3 Response of stream flow to climate change

4.3.1 Annual streamflow change

The potential effect of future climate change in annual streamflow generated by the outputs of the IMP-EMI-LR and CCSM4 models and tow downscaling approaches is shown in Table 6. It realized that, the expected change rate in 2020s, 2050s and 2080s fluctuated between 7.2 and 68.1 %, for the two models when CF approach applied. While, the possible annual streamflow changes in the same period, when the QM method applied is predicted to be ranged between −8.4 and 15.6 %. Whereas under RCP4.5 scenario for the MPI-ESM-LR model, the annual stream flow projected by the two downscaling methods nearly has convergent increase trend. RCP8.5 scenario indicated a different annual streamflow trend fluctuated between 13.9 to 29.0 % and from −8.4 to 6.0 % relative to QM and CF methods respectively. However, the CCSM4 model under CF method was predicted magnificent increase trend in annual streamflow in contrast with QM method. Accordingly, this increment, which predicted by

the CF approach is seemingly due to its high rainfall projection. Despite the projected streamflow varied between increase and decline, the increase trend was the dominate characteristic in streamflow prediction.

4.3.2 Monthly stream flow change

The mean monthly streamflow in 2020s under CCSM4 model and CF approach expected to be changed in June and October from 1.8 to 12.1 $m^3 s^{-1}$ and from 79.6 to 197.5 $m^3 s^{-1}$ respectively and varied with percentage rate ±18 % of baseline period in other months. While monthly streamflow predicted by applying the QM approach to the same model in June and October altered from 1.8 to 99.1 $m^3 s^{-1}$ and from 79.6 to 159.9 $m^3 s^{-1}$ respectively and decreased in other months with percentage range of 67 %. Streamflow projected by IMP-ESM-LR model and CF method showed reasonable variability in June and October from 1.8 to 3.1 $m^3 s^{-1}$ and from 79.6 to 99.7 $m^3 s^{-1}$ respectively and uptrend range of 81 % in all other months as shown in Figs. 6 and 7. However, by applying the QM method, streamflow increased significantly in June and October from 1.8 to 4.9 $m^3 s^{-1}$ and from 79.6 to 126.9 $m^3 s^{-1}$ respectively, while other months were fluctuated within ±31 %. Although the percentage of streamflow increment in 2050 was somewhat less than that of 2020s, the prediction of IMP-ESM-LR and CCSM4 and two approaches generally showed a similar upward trend in the two periods. Similarly to 2020s and 2050s, the Monthly streamflow predictions for future periods 2080s showed the upward trend with a slight difference in the magnitude in some months comparing to baseline period. The high percentage of change in monthly streamflow which displayed by two GCMs under CF and QM approaches may be related to the seasonality of the river. In fact, any alterations in rainfall would result in greater percentage changes in runoff, and this true for monthly discharge values obtained by CF and CCSM4 which dramatically increased in June and October as a result of significant increment of rainfall for the same months generated under the similar method. Despite, RCP8.5 under IMP-EMI-LR and QM approach in 2020s and 2050s showed an increment in rainfall projection; the streamflow is projected to

be decrease. This could be owing to the projection of high temperature increase during this period. Corresponding to IMP-EMI-LR, CCSM4 projected higher increment in streamflow over the study periods may be due to high temperature predicted by the first model.

Based on the results obtained in this study, there is an uncertainty in the simulated streamflow under given climate change conditions, this uncertainty can be attributed to different sources of variability represented in future emissions scenarios, GCMs projections, downscaling approaches and hydrological model parameterization.

4.4 Impact of climate change on DNP ecosystem habitats

4.4.1 Impact of climate change during the drought periods (1960s, 1970s and 1980s)

For the best of our knowledge, the DNP ecosystem has three major components namely woodlands (A. Seyal-Balanites), River stream and the Mayas (Wetlands). Moreover, DNP ecosystem provides sustainable habitations for many species of Flora and Fauna, which they live or spend in it a part of essential key stages of their annual life cycle. Precisely, River stream and the Mayas which offer sustainable refuge and protection for the Living organisms after the flood season, they consider as a valuable store for that reactive link to keep on their flora and fauna existence until the next flood start and recharge the pools and Mayas (Hakim et al., 1978; Abdel Hameed and El-jack, 2003). It should be mentioned that the whole African countries during the last five decades exposed to drought periods, which started in the 1960s and reached the peak in 1984. These drought, consequently, affected every Africa environmental systems; in particular, Sudan and Ethiopia (Mattsson and Rapp, 1991; Elagib and El-hag, 2011; Masih et al., 2014). Thus, climate change had pronounced effects on the DR stream and the Mayas through changed precipitation and occurrence of drought waves. The hugely impact of the drought intervals caused significant variability in the water level in DR and the Mayas during the flood season. These changes could be

the main agent in the wetlands ecosystem alteration, and accordingly influenced all the ecosystem components. This consistent with Woo et al. (1993) who pointed out that, the fate of the wetlands under climate change is mainly depending to changes in external recharge, which related to alterations in precipitation and evaporation over the wetland itself. Moreover, comparatively tiny increments in precipitation change can significantly influence wetlands Flora and Fauna at various phases of their lives' cycle (Keddy, 2000). As a result, the entire wetland's ecosystem was affected by alterations in precipitation and streamflow (Bauder, 2005). Therefore, according to the seasonality of the DR, small decrease or increase in the annual rainfall leads to decline or increment the water level, and the impact will extend to the next seasons as happened during the drought periods. The rainfall over DRB during the first drought period (1963 and 1965) and (1969 to 1972) declined about 23 and 11 %, respectively, which led to decline the runoff about 47 % during (1972 to 1977). The second wave of drought started in 1978 to 1987 that decreased the rainfall about 14.8 %, led to decrease the runoff about 20 %. These alterations caused a sharp decline in the DR runoff and seriously affected the water availability in many Mayas. Moreover, the waves of drought followed by a flood season led to the remarkable damage in the river stream by closing the channels' feeder from the main stream to Mayas and increasing the erosion and sedimentation. Consequently, it decreased the water amounts and many of Mayas dried. There are about 40 Mayas distributed in the DNP such as Ras Amir, Gadahat, and Godah influenced by alterations in the rainfall trend during drought periods. Ras Amir considers as the largest Maya (4.5 km^2), was dried up during the drought periods (1970) and since that time became less enduring, haphazardly every few years, and full of water in other years. Farash el Naam is the second biggest Maya (1.6 km^2) after drought periods (1980) became more inconstant and lesser eternal. The last one is Godaha, consists of a series of eleven small Mayas; Godahat is the major one (0.2 km^2), which was affected by the drought period as well (Hakim et al., 1978; Abdel Hameed, 1983; Abdel Hameed et al., 1997; Abdel Hameed and Eljack, 2003). Thus, changes in temperature, precipitation and streamflow magnitude affected the sustainability of ecosystem

in terms of the components' habitats in the DNP. Consequently, the damage in habitats impacted most of the flora and fauna in the DNP.

In this century, DNP habitats virtually certain expose to the climate change impact, such as temperature increment or rainfall increase and/or decline, which will very likely affect the flora and fauna and their migration, blooming and mating timing.

4.4.2 Impact of projected climate change on DNP ecosystem habitats

Based on the climate change projections' scenarios, the changes in temperature and precipitation will impact either directly or indirectly the streamflow magnitude. Consequently, the DNP ecosystem will very likely be exposed to a variety of negative and positive effects based on these projections. Although climatic warming in this century is expected to start a drying trend in wetland ecosystems in most parts of the world (Gorham, 1991), the results obtained by this work accomplished that the DRB wetlands will experience increment in water magnitude according to the projected increment in the annual streamflow. Generally, the temperature increase and greater changes in precipitation will occur in DNP over this century. The IMP-ESM-LR and CCSM4 models projected annually increases in T_{max} ranged from 0.9 to 4.9 °C and T_{min} ranged from 0.9 to 5 °C; the RCP8.5 scenario projected the greatest increase. Alterations in precipitation are projected to vary in spatially and temporally when CF and QM approaches applied between 1.8 to 32.8 % and between 6.2 to 21.4 % respectively. DNP is expected to get drier in the summer, whereas more likely to be wetter in autumn. The rainfall increment will be greater in the southeast part of DNP more than the northwest. Moreover, the intensity and the maximum magnitude of precipitation, will likely increase as well.

The upward trend in the rainfall amount which predicted by two models will have distinctive positive impacts on the DNP ecosystems in terms of habitat sustainability of many Living organisms. The IMP-ESM-LR and CCSM4 models when CF and QM approaches applied, projected increase in rainfall over DRB ranged between 1.5 to 42.4 % and between 6.2 to 15.8 % respectively, which will likely lead to an increment

in streamflow ranged between 7.2 to 68.1 % and between 3.4 to 15.6 % in the 2020s, 2050s and 2080s. These increases in the streamflow likely will be suitable amounts to restoration of the DNP ecosystem components. Despite, the rainfall increment projected by CCSM4 apparently does not affect DNP ecosystem positively, the predicted rainfall pattern is totally different from the baseline period among rainy months. This might lead to positive effect on the distribution of the water amount in flood season, which will increase water availability duration. DNP lies on the road of winter migration for many African birds during their pass to eastern Africa Rift valley lakes or southward. Accordingly, the increase of water during the flood season in this century will lead to increase the capacity of the Mayas and pools to receive more numbers of these migrant birds. Furthermore, these habitats will not be a breed effective threat and danger on the life cycle for that birds and defect on the ecosystem balance of DNP and regional scale. Otherwise almost the two GCMs predictions indicated that precipitation most probably tends to increase in the future over the DNP. Consequently, this positive variation will likely greatly influence the water level in Mayas and pools and promote the intensity of vegetation cover and growing of the grasses which consider a major food source for most DNP fauna.

On the other hand, the increment in precipitation intensity will likely increase the frequency of flooding, and landslides. This will likely generate increased rates of erosion and sedimentation, which causing a decrease of supply from stream channel banks to the wetlands and the capacity. As stated in the two GCMs scenarios, which projected significant annually and monthly increment in temperature. This increment will likely affect the habitats' component in the DNP, as the water level will be affected by the evapotranspiration over the DRB, particularly under The IMP-ESM-LR model and RCP8.5 scenario at the end of this century.

According to the projected alterations in the temperature, precipitation and streamflow, we expected that DNP ecosystem' events, and habitats will very likely to be shifted. In fact, the temperature and precipitation over DNP varied spatially and temporally. The annual precipitation increases about 30 mm every 10 km from the northwest

to the southeast (Ethiopian Plateau), while the temperature decreases with the rainfall increase. This offers DNP ecosystem the same habitat with different climatic conditions (temperature and precipitation). Consequently, most of the fauna and flora have high resilience to adapt to the impact of the climate change and habitats' loss as happened during drought periods. This implies that, during drought periods some of the fauna and flora have changed their habitats to the areas that have the same climate conditions of their previous habitats as a form of adaptation. Furthermore, over the last 100 years, maximum temperature with mean rainfall as secondary driver was the determinant factor in habitat loss and fragmentation, averaged across species and geographic regions. Habitat loss and fragmentation effects were greatest in areas with high maximum temperatures. Conversely, they were lowest in areas where average rainfall has increased over time (Mantyka-pringle et al., 2012). Based on the projected climate determinants and DNP ecosystem characteristics, we inferred that, ecosystem components will likely expect to start restoration of ecosystem habitats.

5 Conclusion

The study analyzed the response of streamflow and ecosystem habitats in the DRB to possible future climate conditions change that predicted by using two GCMs coupled with two downscaling approaches and physically based distributed hydrologic model (SWAT). Predictions of two GCMs pointed out the temperature and precipitation will increase in the next century. Consequently, streamflow is likely will increase according to rainfall increase. Type of the used downscaling approach was a key factor in climatic variables' projection. The annual rainfall predicted by QM approach based on two GCMs tend to have the same increasing trend, particularly under RCP4.5 scenario. The CF approach showed huge increment with CCSM4 compare by IMP-ESM-LR. In contrast, the IMP-ESM-LR model under both CF and QM approaches in RCP8.5 scenario, predicted convergent annual rainfall upward trend, whereas it varied for the RCP4.5 scenario. The similarity of the result obtained by QM under the two GCMs models was

regarded to the fact that the QM approach taken into account daily rainfall time series generated by the GCM. There is uncertainty in the Streamflow projection basically depended on the GCMs, scenarios, downscaling approach and model parameterization. Relying on prediction of potential possible changes in climate condition, ecosystem components in DNP substantially will likely be affected in a way that make that living organism habitats and life cycle will likely have recovery conditions rather than extinction and destruction circumstances, as it was happening during drought periods (1960s, 1970s and 1980s). On the other hand, the projected rainfall and the seasonality of the river will make more uneven distribution of annual flow from year to another. Thus, high attentions to extreme events (floods and drought) to avoid the negative hydrological effect on the DNP ecosystem habitats should be considered. The presented study projected the hydroclimatic condition over DNP and assessed how ecosystem habitats respond to the changes of these variables. The results provide benchmark information that can be used to increase the capacity of the water resources management and ecosystem conservation strategies through identify suitable actions for the future. That is to create more resilience to climate changes related to habitats restoration and continued management of other stressors in DNP ecosystem. Furthermore, integrity of hydrological conditions in DR stream and Mayas' should be considered, to reduce the negative impact of climate change on fragmented wetlands' ecosystem, practically in terms of drought and sediments.

References

Abbaspour, K. C., Yang, J., Maximov, I., Siber, R., Bogner, K., Mieleitner, J., Zobrist, J., and Srinivasan, R.: Modelling hydrology and water quality in the pre-alpine/alpine Thur watershed using SWAT, J. Hydrol., 333, 413–430, 2007.

Abdel Hameed, S. M.: Vegetation of the Mayas of Dinder National Park, Colorado State University, Sudan, 1983.

Abdel Hameed, S. M. and Eljack, A. O.: Ramsar Information Sheet (RIS) for Dinder national park, Sudan, Wetlands International Global, available at: https://rsis.ramsar.org/RISapp/files/RISrep/SD1461RIS.pdf (last access: 1 April 2015), 2013.

AbdelHameed, S. M., Awad, N. M., ElMoghraby, A. I., Hamid, A. A., Hamid, S. H., and Osman, O. A.: Watershed management in the Dinder National Park, Sudan, Agr. Forest Meteorol., 84, 89–96, 1997.

Bauder, E.: The effects of an unpredictable precipitation regime on vernal pool hydrology, Freshwater Biol., 50, 2129–2135, 2005.

Burkett, V. R., Wilcox, D. A., Stottlemyer, R., Barrow, W., Fagre, D., Baron, J., Price, J., Nielsen, J. L., Allen, C. D., and Peterson, D. L.: Nonlinear dynamics in ecosystem response to climatic change: case studies and policy implications, Ecol. Complex., 2, 357–394, 2005.

Camici, S., Brocca, L., Melone, F., and Moramarco, T.: Impact of climate change on flood frequency using different climate models and downscaling approaches, J. Hydrol. Eng., 19, 04014002, doi:10.1061/(ASCE)HE.1943-5584.0000959, 2013.

Charlton, R., Fealy, R., Moore, S., Sweeney, J., and Murphy, C.: Assessing the impact of climate change on water supply and flood hazard in Ireland using statistical downscaling and hydrological modelling techniques, Climatic Change, 74, 475–491, 2006.

Chow, V. T., Maidment, D. R., and Mays, L. W.: Applied Hydrology, McGraw-Hill Series in Water Resources and Environmental Engineering, McGraw-Hill, New York, 572 pp., 1988.

Dasmann, W.: Development and management of Dinder National Park and its Wildlife, Rep. 3113, Food and Agriculture Organisation, Rome, Italy, 2–62, 1972.

Dessu, S. B. and Melesse, A. M.: Impact and uncertainties of climate change on the hydrology of the Mara River basin, Kenya/Tanzania, Hydrol. Process., 27, 2973–2986, 2013.

Diaz-Nieto, J. and Wilby, R. L.: A comparison of statistical downscaling and climate change factor methods: impacts on low flows in the River Thames, UK, Climatic Change, 69, 245–268, 2005.

Döll, P. and Zhang, J.: Impact of climate change on freshwater ecosystems: a global-scale analysis of ecologically relevant river flow alterations, Hydrol. Earth Syst. Sci., 14, 783–799, doi:10.5194/hess-14-783-2010, 2010.

Elagib, N. A. and Elhag, M. M.: Major climate indicators of ongoing drought in Sudan, J. Hydrol., 409, 612–625, 2011.

Erwin, K. L.: Wetlands and global climate change: the role of wetland restoration in a changing world, Wetl. Ecol. Manage., 17, 71–84, 2009.

Ficklin, D. L., Luo, Y., Luedeling, E., Gatzke, S. E., and Zhang, M.: Sensitivity of agricultural runoff loads to rising levels of CO_2 and climate change in the San Joaquin Valley watershed of California, Environ. Pollut., 158, 223–234, 2010.

Finlayson, C. M., Gitay, H., Bellio, M. G., van Dam, R. A., and Taylor, I.: Climate variability and change and other pressures on wetlands and waterbirds: impacts and adaptation, Waterbirds Around the World, edited by: Boere, G. C., Galbraith, C. A., and Stroud, D. A., The Stationery Office, Edinburgh, 88–97, 2006.

Fowler, H., Blenkinsop, S., and Tebaldi, C.: Linking climate change modelling to impacts studies: recent advances in downscaling techniques for hydrological modelling, Int. J. Climatol., 27, 1547–1578, 2007.

Gitay, H., Suárez, A., Watson, R. T., and Dokken, D. J.: Climate Change and Biodiversity, Intergovernmental Panel on Climate Change, IPCC Technical Paper V, 77 pp., IPCC, Geneva, 2002.

Gorham, E.: Northern peatlands: role in the carbon cycle and probable responses to climatic warming, Ecol. Appl., 1, 182–195, 1991.

Hakim, S., Fadlalla, B., Awad, N. M., and Wahab., S. A.: Ecosystems of the vegetation of Dinder national park, Unpublished report, Wildlife Research Unit, Khartoum, Sudan, 1978.

Hay, L. E., Wilby, R. L., and Leavesley, G. H.: A comparison of delta change and downscaled GCM scenarios for three mounfainous basins in the United States, Jawra, J. Am. Water Resour. As., 36, 387–397, 2000.

Mantyka-pringle, C. S., Martin, T. G., and Rhodes, J. R.: Interactions between climate and habitat loss effects on biodiversity: a systematic review and meta-analysis, Global Change Biol., 18, 1239–1252, 2012.

Masih, I., Maskey, S., Mussá, F. E. F., and Trambauer, P.: A review of droughts on the African continent: a geospatial and long-term perspective, Hydrol. Earth Syst. Sci., 18, 3635–3649, doi:10.5194/hess-18-3635-2014, 2014.

Title Page

Abstract | Introduction

Conclusions | References

Tables | Figures

◄ | ►

◄ | ►

Back | Close

Full Screen / Esc

Printer-friendly Version

Interactive Discussion

Mattsson, J. O. and Rapp, A.: The recent droughts in western Ethiopia and Sudan in a climatic context, Ambio, 20, 172–175, 1991.

Millennium Ecosystem Assessment: Ecosystems and Human Well-being: Biodiversity Synthesis, Island Press, Washington, D.C., 2005.

5 Moriasi, D., Arnold, J., Van Liew, M., Bingner, R., Harmel, R., and Veith, T.: Model evaluation guidelines for systematic quantification of accuracy in watershed simulations, T. ASABE, 50, 885–900, 2007.

Nash, J. and Sutcliffe, J. V.: River flow forecasting through conceptual models part I – a discussion of principles, J. Hydrol., 10, 282–290, 1970.

10 Neitsch, S., Arnold, J., Kiniry, J., Srinivasan, R., and Williams, J.: Soil and Water Assessment Tool User's Manual: Version 2000, GSWRL Report 02-02, BRC Report 02-06, Publ. Texas Water Resources Institute, TR-192, College Station, Texas, 2002.

Neitsch, S., Arnold, J., Kiniry, J., Srinivasan, R., and Williams, J.: Soil and Water Assessment Tool Input/Output File Documentation, Blackland Research Center, Temple, Texas, 2005a.

15 Neitsch, S., Arnold, J., Kiniry, J., Williams, J., and King, K.: Soil and Water Assessment Tool Theoretical Documentation, Grassland, Soil and Water Research Laboratory, Temple, Texas, 2005b.

Poff, N. L. and Ward, J. V.: Implications of streamflow variability and predictability for lotic community structure: a regional analysis of streamflow patterns, Can. J. Fish. Aquat. Sci., 46, 20 1805–1818, 1989.

Poff, N. L. and Zimmerman, J. K.: Ecological responses to altered flow regimes: a literature review to inform the science and management of environmental flows, Freshwater Biol., 55, 194–205, 2010.

Sennikovs, J. and Bethers, U.: Statistical downscaling method of regional climate model results 25 for hydrological modelling, in: Proc. 18 World IMACS/MODSIM Congress, Cairns, Australia, 2009.

Setegn, S. G., Rayner, D., Melesse, A. M., Dargahi, B., and Srinivasan, R.: Impact of climate change on the hydroclimatology of Lake Tana Basin, Ethiopia, Water Resour. Res., 47, W04511, doi:10.1029/2010WR009248, 2011.

30 Steele-Dunne, S., Lynch, P., McGrath, R., Semmler, T., Wang, S., Hanafin, J., and Nolan, P.: The impacts of climate change on hydrology in Ireland, J. Hydrol., 356, 28–45, 2008.

Tavakoli, M. and De Smedt, F.: Impact of climate change on streamflow and soil moisture in the Vermilion Basin, Illinois, J. Hydrol. Eng., 17, 1059–1070, doi:10.1061/(ASCE)HE.1943-5584.0000546, 2011.

Teutschbein, C. and Seibert, J.: Bias correction of regional climate model simulations for hydrological climate-change impact studies: review and evaluation of different methods, J. Hydrol., 456, 12–29, 2012.

Thom, H. C.: A note on the gamma distribution, Mon. Weather Rev., 86, 117–122, 1958.

Thomas, C. D., Cameron, A., Green, R. E., Bakkenes, M., Beaumont, L. J., Collingham, Y. C., Erasmus, B. F., De Siqueira, M. F., Grainger, A., and Hannah, L.: Extinction risk from climate change, Nature, 427, 145–148, 2004.

Whiteman, A.: Tho Geology of the Sudan Republic, Clarendon Press, Oxford University Press, London, 1971.

Wilby, R. L., Dawson, C. W., and Barrow, E. M.: SDSM – a decision support tool for the assessment of regional climate change impacts, Environ. Model. Softw., 17, 145–157, 2002.

Woo, M.-K., Rowsell, R. D., and Clark, R. G.: Hydrological classification of Canadian prairie wetlands and prediction of wetland inundation in response to climatic variability, Occasional Paper No. 79, Canadian Wildlife Service, Saskatoon, Canada, 1–24, 1993.

Xu, C.-Y.: Climate change and hydrologic models: a review of existing gaps and recent research developments, Water Resour. Manage., 13, 369–382, 1999.

Table 1. Information of coupled climate models.

Model name	Model centre	Resolution
MPI-ESM-LR	Max-Planck-Institute for Meteorology, Hamburg, Germany	$1.875° \times 1.875°$
CCSM4	the National Centre for Atmospheric Research, USA	$1.25° \times 0.9375°$

Table 2. Calibration (1989–1993) and validation (1995–1999) of SWAT model.

Period	NS	R2
Monthly		
Calibration (1989–1993)	0.81	0.83
Validation (1995–1999)	0.76	0.82
Daily		
Calibration (1989–1993)	0.62	0.63
Validation (1995–1999)	0.51	0.56

Table 3. Annual changes in T_{max} in the future under two GCMs and two scenarios (RCP4.5 and RCP8.5) at the upstream positions of the DRB.

| Period's Annual change in T_{max} (°C) | | |
MPI-ESM-LR	CCSM4	
RCP4.5		
2020s	1.4	0.9
2050s	2.4	1.5
2080s	3.0	1.7
RCP8.5		
2020s	1.6	1.0
2050s	2.9	1.9
2080s	4.9	3.5

Table 4. Annual changes in T_{min} in the future under two GCMs and two scenarios (RCP4.5 and RCP8.5) at the upstream portions of the DRB.

Period's Annual change in T_{min} (°C)		
	MPI-ESM-LR	CCSM4
RCP4.5		
2020s	1.4	0.9
2050s	2.4	1.6
2080s	2.9	1.7
RCP8.5		
2020s	1.6	0.9
2050s	3.0	1.9
2080s	5.1	3.4

Table 5. Annual changes in precipitation in the future under RCP4.5 and RCP8.5 scenarios at the upstream portions of the DRB.

Period's Annual change in precipitation (%)			
Change factor method		Qunatile method	
MPI-ESM-LR	CCSM4	MPI-ESM-LR	CCSM4
RCP4.5			
2020s	2.3	40.4	6.5	6.9
2050s	1.5	35.3	6.5	6.7
2080s	3.0	28.1	7.8	11.1
RCP8.5			
2020s	4.6	42.5	6.5	10.5
2050s	9.2	39.7	8.7	16.4
2080s	10.5	36.2	14.9	13.9

Table 6. Possible annual streamflow changes in the future years (2020s, 2050s and 2080s) at the upstream portions of the DRB.

Period's Annual change in streamflow (%)				
	Change factor method		Qunatile method	
	MPI-ESM-LR	CCSM4	MPI-ESM-LR	CCSM4
RCP4.5				
2020s	10.5	68.1	8.1	13.7
2050s	7.2	59.3	3.4	11.3
2080s	13.2	63.5	6.1	14.0
RCP8.5				
2020s	13.9	66.9	−2.8	13.3
2050s	22.6	53.0	−8.4	15.6
2080s	29.0	67.8	6.0	11.4
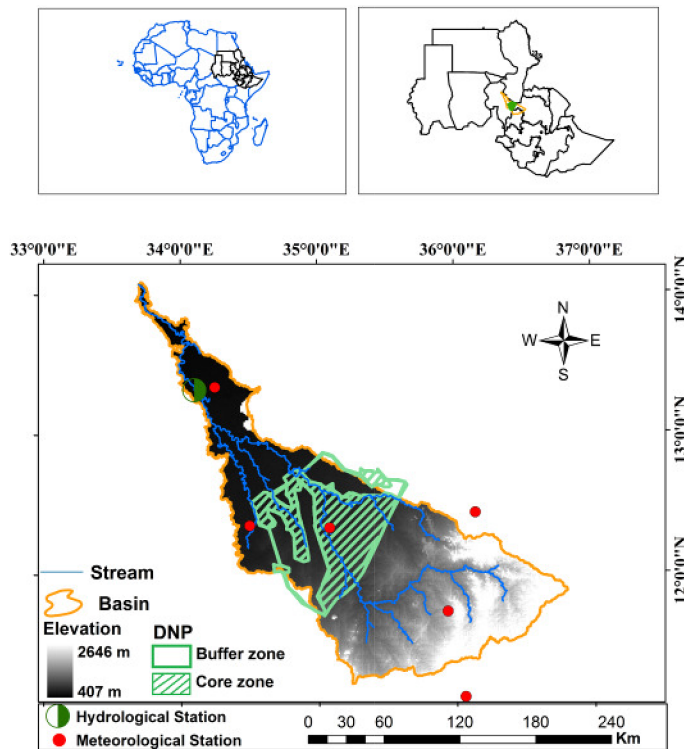
Figure 1. Topography (m) of the Dinder River basin based on a 90 km digital elevation model and geographic locations of DNP and hydrological and meteorological stations.
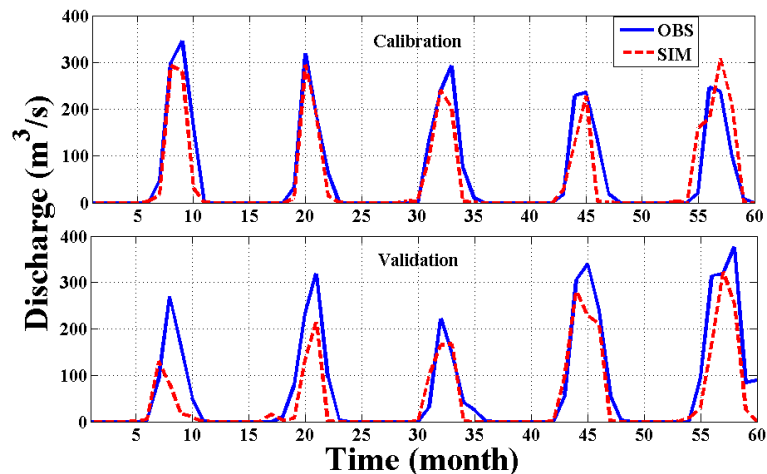
Figure 2. SWAT simulated and observed monthly stream flow in Al Gwisi gauges during the calibration period (1989–1993) (upper panel) and validation period (1995–1999) (lower panel), OBS indicates the observed flow and SIM indicates to simulated flow.
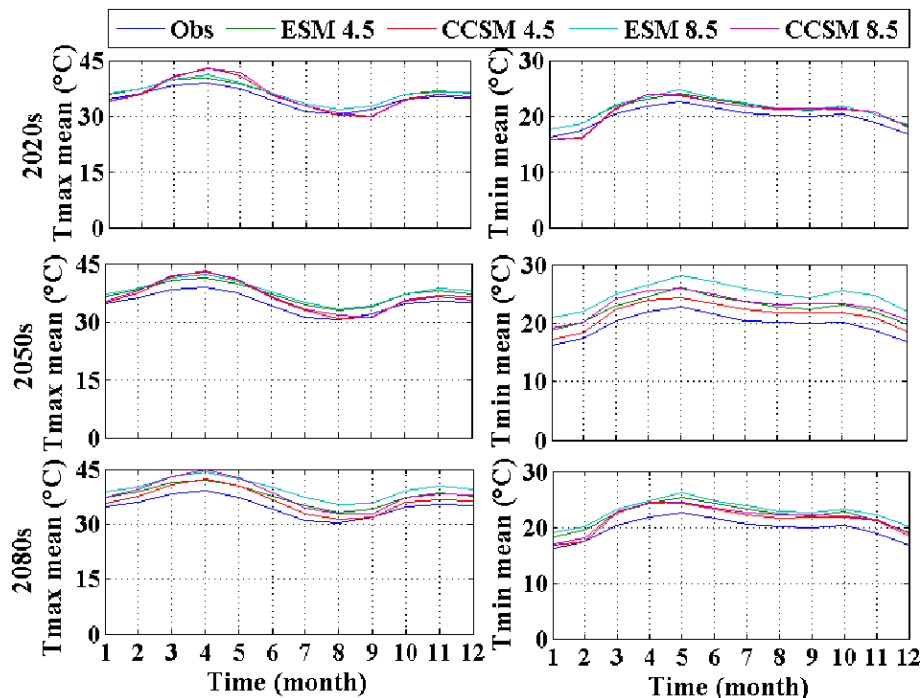
Figure 3. Observed and predicted mean temperature (T_{max} and T_{min}) of the baseline years (1980s) and the future years (2020s, 2050s and 2080s) at the upstream portions of the DRB.

Full Screen / Esc
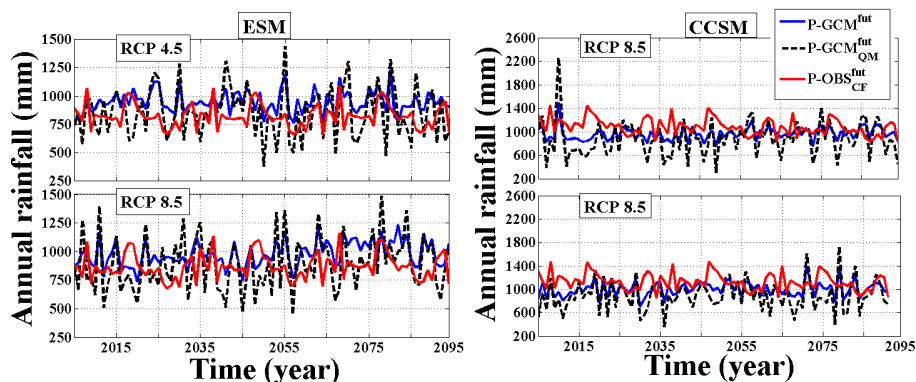
Figure 4. Comparison between the annual rainfall data for future periods provided by the MPI-ESM-LR (right panel) and CCSM4 (left panel) models, before (blue line) and after (red and black line) the application of the CF and QM approaches.
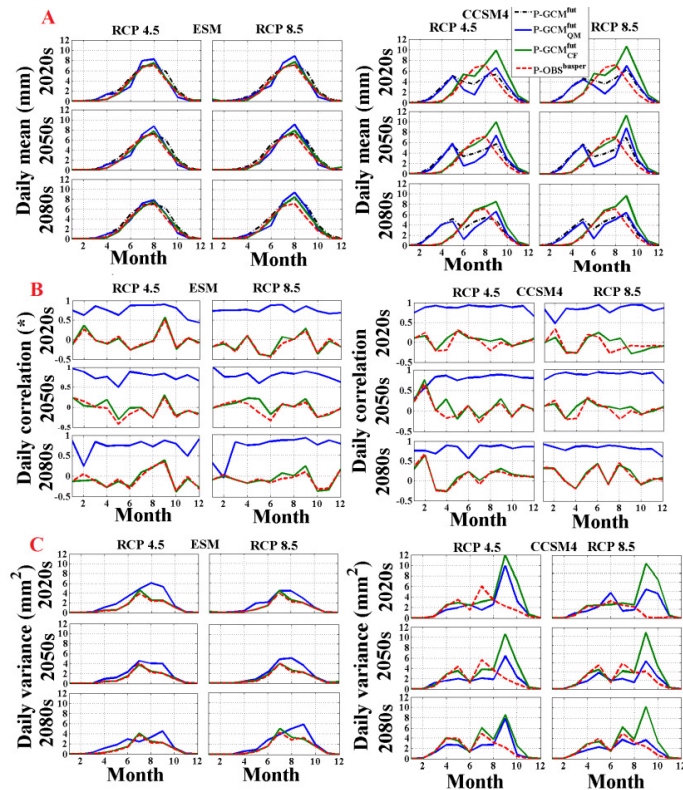
Figure 5. MPI-ESM-LR and CCSM4 model results over the DRB. Comparison at monthly level between the statistical properties of the GCMs outputs data downscaled with the CF(P-OBS$_{CF}^{fut}$) and QM(P-GCM$_{QM}^{fut}$) approaches. The observed data for the baseline period (P-OBS^{basper}) are also shown to assess the impact of climate changing.
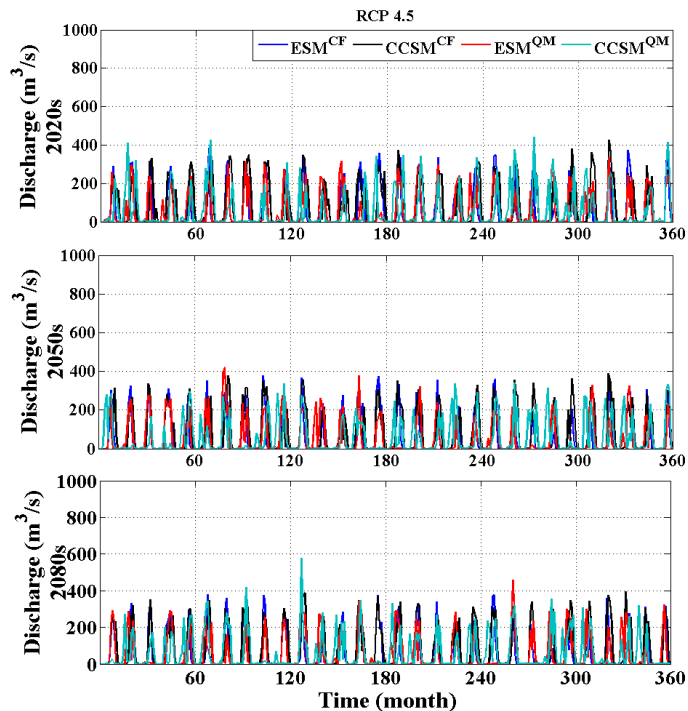
Figure 6. Possible monthly streamflow change (2020s, 2050s and 2080s) at the upstream portions of the DRB for MPI-ESM-LR and CCSM4 models when two downscaling (QM and CF) methods applied (ESM^{QM}, ESM^{CF}) and (CCSM4^{QM}, CCSM4^{CF}).
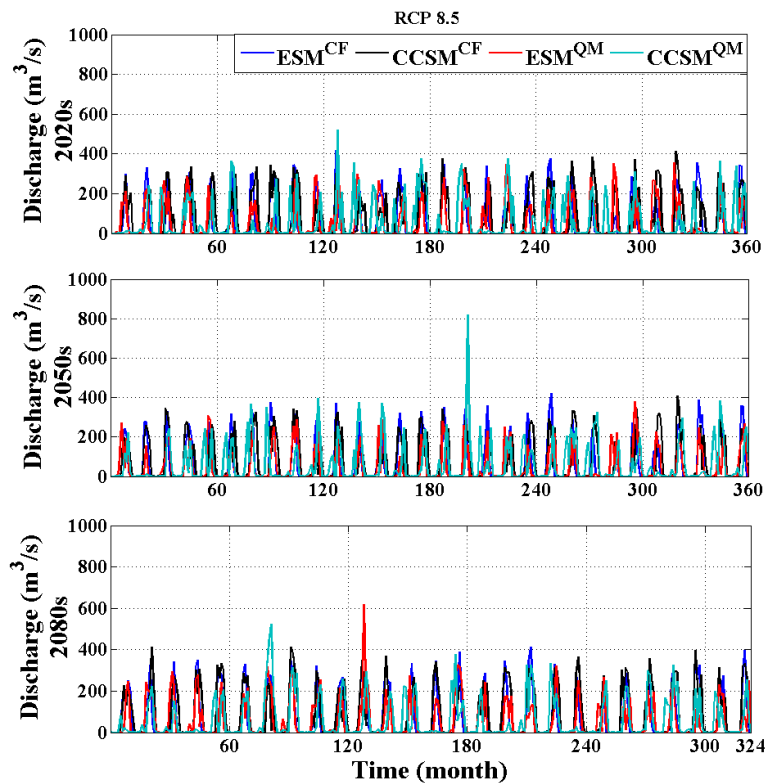
Figure 7. As in Fig. 6, but for the RCP8.5 scenario.

Full Screen / Esc

Printer-friendly Version

Interactive Discussion